Solar Energy
And Sustainable Development
Refereed, biannual scientific journal issued by:
The Libyan Center for Solar Energy Research and Studies

2D/2D GO-Modified g-C_3N_4 Nanocomposite for Efficient Photocatalytic CO_2 Reduction to CH_4 Under Visible Light

Riyadh Ramadhan Ikreedeegh[1,2,3*], Md. Arif Hossen[4,5], Muhammad Tahir[1].

[1]Chemical and Petroleum Engineering Department, UAE University, Al Ain, United Arab Emirates.
[2]Department of Analysis and Quality Control, Sarir Oil Refinery, Arabian Gulf Oil Company, Benghazi, Libya.
[3]Libyan Advanced Center for Chemical Analysis, Libyan Authority for Scientific Research, Tripoli, Libya.
[4]Faculty of Civil Engineering Technology, Universiti Malaysia Pahang Al-Sultan Abdullah, Pahang, Malaysia.
[5]Institute of River, Harbor and Environmental Science, Chittagong University of Engineering and Technology, Chattogram, Bangladesh.

E-*mail:* riyadhkridiegh@gmail.com , muhammad.tahir@uaeu.ac.ae .

ARTICLE INFO.

Article history:
Received 4 Jul 2024
Received in revised form 7 Jul 2024
Accepted 19 Sep 2024
Available online 28 Sep 2024

KEYWORDS

Carbon-based nanomaterials; 2D/2D nanostructure; Photocatalytic CO_2 reduction; CH_4 production; Solar fuels.

ABSTRACT

Polymeric graphitic phase carbon nitride (g-C_3N_4) photocatalysts offer significant potential for CO_2 photoreduction into solar fuels despite their efficiency restricted due to poor light response and recombination of photo-generated charges. This study focused on the modification of g-C_3N_4 by single-layered graphene oxide (GO) for enhancing photocatalytic CO_2 reduction activity to form CH4. Well-designed 2D/2D GO-g-C_3N_4 was fabricated using facile thermal strategy.

The hybrid photocatalyst exhibited improved CO_2 photoreduction performance to produce CH_4. The maximum CH_4 yield of 25.61 µmol g-1 was achieved after 4 h of visible light illumination which represents about 25% enhancement compared to pristine g-C_3N_4.

The incorporation of GO co-catalyst not only facilitates charge transfer but also offers an ample number of catalytic sites for CO_2 adsorption. This work showcased the fabrication of g-C_3N_4-based binary photocatalyst with high CO_2 photoreduction efficiency by coupling with metal-free co-catalyst.

*Corresponding author.

DOI: https://doi.org/10.51646/jsesd.v13i2.218

مركب الـ g-C_3N_4 النانوي ثنائي الأبعاد والمُعدل بواسطة الـ GO لتحويل ثاني أكسيد الكربون إلى CH_4 بكفاءة عن طريق التحفيز الضوئي تحت الضوء المرئي

رياض رمضان كريديغ، محمد عريف، محمد طاهر .

ملخص: توفر مُحفزات نيتريد الكربون الضوئية ذات الطور الجرافيتي البوليمري (g-C_3N_4) إمكانات كبيرة لإختزال وتحويل ثاني أكسيد الكربون ضوئيًا إلى وقود الطاقة الشمسية على الرغم من تقييد كفاءتها بسبب ضعف الاستجابة للضوء وإعادة تركيب الشحنات المولدة ضوئياً. ركزت هذه الدراسة على تعديل الـ g-C_3N_4 بواسطة أكسيد الجرافين (GO) أحادي الطبقة لتحسين كفاءة تحويل ثاني أكسيد الكربون بالتحفيز الضوئي إلى غاز الميثان (CH_4). تم تصنيع مركب الـ g-C_3N_4/GO ثنائي الأبعاد ذو التصميم الجيد باستخدام إستراتيجية حرارية بسيطة. أظهر المُحفز الضوئي الهجين أداءً محسنًا في التحويل الضوئي لثاني أكسيد الكربون إلى غاز الميثان. تم تحقيق أعلى إنتاج من الميثان والبالغ 25.61 ميكرومول/جم بعد تسليط الضوء المرئي لمدة 4 ساعات والذي يمثل زيادة بنسبة 30% تقريبًا مقارنة بالـ g-C_3N_4 النقي. دمج محفز الـ GO المساعد لا يؤدي إلى تسهيل نقل الشحنات فحسب، بل يوفر أيضًا عددًا كبيرًا من المواقع المُحفزة لإمتزاز غاز ثاني أكسيد الكربون. أظهر هذا العمل التطوير الجديد للمُحفزات الضوئية الثنائية والمُعتمدة على الـ g-C_3N_4 وذات الكفاءة العالية في التحويل الضوئي لثاني أكسيد الكربون من خلال الدمج مع مُحفزات مساعدة خالية من المعادن.

الكلمات المفتاحية – المواد النانوية القائمة على الكربون، البُنية النانوية ثنائية الأبعاد، تخفيض ثاني أكسيد الكربون بالتحفيز الضوئي، إنتاج الميثان، وقود الطاقة الشمسية.

1. INTRODUCTION

Since the beginning of the current century and owing to the booming industrial sector, energy shortage and atmospheric pollution issues have become progressively prominent. Hence, applying green technology to capture and transform CO_2 into solar fuels can reduce reliance on fossil fuels while simultaneously lowering the atmospheric amounts of CO_2 gas and solving the issue of environmental pollution [1–3]. The photocatalytic (PC) CO_2 reduction approach has been regarded as one of the most promising CO_2 utilization technologies among the other CO_2 utilization strategies [4–8]. However, the rapid recombination of photo-excited charge carriers, limited CO_2 adsorption capacity, sluggish rate of electrons transfer, and inadequate surface-active sites have greatly hindered the entire photoconversion efficiency [9–11]. Researchers are striving to find an efficient and suitable strategy to improve the CO_2 photoreduction rate.

In the recent past, semiconductor photocatalysts have been extensively explored for enhancing the performance of CO_2 photo-reduction. The class of metal-free polymers more specifically graphitic phase carbon nitride (g-C_3N_4) has captured stimulated attention for PC CO_2 reduction because of its facile and affordable fabrication method, visible light response and diverse hierarchical structures [12–14]. However, the CO_2 photo-reduction rate of pure g-C_3N_4 is usually limited to laboratory scale due to moderate bandgap energy (2.7 eV) and fast recombination of photo-generated charge carriers. Recent studies reported enhanced CO_2 photoreduction efficiency over modified g-C_3N_4 heterostructures. For instance, Guo et al. [15] modified g-C_3N_4 by porous ZnO to enhance PC CO_2 reduction efficiency. The constructed ZnO@g-C_3N_4 hybrid photocatalysts exhibited 3.06 times higher CH_4 production than bare g-C_3N_4. The incorporation of gold (Au) noble metal with ZnO and g-C_3N_4 by Li and coworkers [16] demonstrated 4.5 times higher CO production than pristine g-C_3N_4 owing to the localized surface plasmon resonance (LSPR) effect. Recently, modification of g-C_3N_4 by H_3PO_4 showed 4.38 times improved photoreduction performance to CO than that of bare g-C_3N_4 under the exposure of visible light [17].

Graphene oxide (GO) is a novel 2D nanomaterial with a single-layer carbon nanosheet of hexagonal structure, which offers great potential for anchoring the g-C_3N_4 with high stability. Furthermore, GO, which has a wide surface area and strong electron mobility, can act as a metal-

free co-catalyst to improve the CO_2 photo-reduction performance by providing more active sites and facilitating the charges transfer [12, 18, 19]. Motivated by this, and to enhance CO_2 photo-reduction efficiency even further, we presented a detailed procedure to fabricate a binary 2D/2D g-C_3N_4/GO photocatalyst that converts the CO_2 gas into CH_4. The newly constructed 2D/2D GO-g-C_3N_4 composite exhibited enhanced PC CO_2 reduction performance, revealing its great potential as an efficient promising photocatalyst. Broadly, the findings of this study provide new insights for the development of low-cost and efficient hybrid nanomaterials for environmental remediation and energy production applications.

2. EXPERIMENTAL SECTION

2.1. Chemicals and Materials

The chemicals used for the synthesis of g-C_3N_4, GO and g-C_3N_4/GO composite were melamine (99.9%, Merck), graphite flakes (99.9%, Sigma Aldrich), potassium permanganate (99%, Merck), sulphuric acid (97 %, Merck), phosphoric acid (99%, Sigma Aldrich), methanol (99.9%, Merck) and deionized water. All chemicals and materials were used as purchased without any further purification.

2.2. Preparation of g-C_3N_4

The g-C_3N_4 was synthesized through the direct heating of melamine powder (10 g) in a muffle furnace at 550 °C for 2 h as reported in previous works [13]. The melamine powder is placed in a covered porcelain crucible and then pyrolyzed until a yellowish bulk material is obtained. The obtained material is then left to cool down to room temperature and crushed into fine powder using a mortar and pestle.

2.3. Preparation of GO

A modified Tour's method was used for preparing the GO nanosheets. Briefly, a small amount of graphite flakes (3 g) was dispersed into a mixture of H2SO4 (360 mL) and H_3PO_4 (40 mL) using a magnetic stirrer operating at 300 rpm. An ice bath was employed for keeping the temperature below 10 °C during the oxidation of graphite flakes. A specific amount of KMnO4 (18 g) was then introduced gradually in which the mixture temperature is maintained less than 50 °C. After 24 h of continuous stirring, a yellowish suspension is obtained to be then cooled and altered by adding H_2O_2 (5 mL) dropwise till a brownish suspension is obtained. Finally, the brownish suspension is filtered, rinsed with distilled water, exfoliated using ultrasonic treatment and dried for 12 h at 50 °C so that GO nanosheets with single layered structure are obtained.

2.4. Preparation of g-C_3N_4/GO nanocomposite

The g-C_3N_4/GO nanocomposite was prepared through a facile thermal approach. Specific amounts of the as-synthesized g-C_3N_4 powder were dispersed in methanol solution (50 mL). Then, the GO powder with different contents (0.25, 0.5, 1 and 2 wt.%) was mixed with the g-C_3N_4/methanol solution under magnetic stirring for 6 h. Finally, the solution was sonicated for 1 h and dried at 100 °C for 12 h. Figure 1 demonstrates the whole synthesis procedure of the g-C_3N_4/GO nanocomposite.

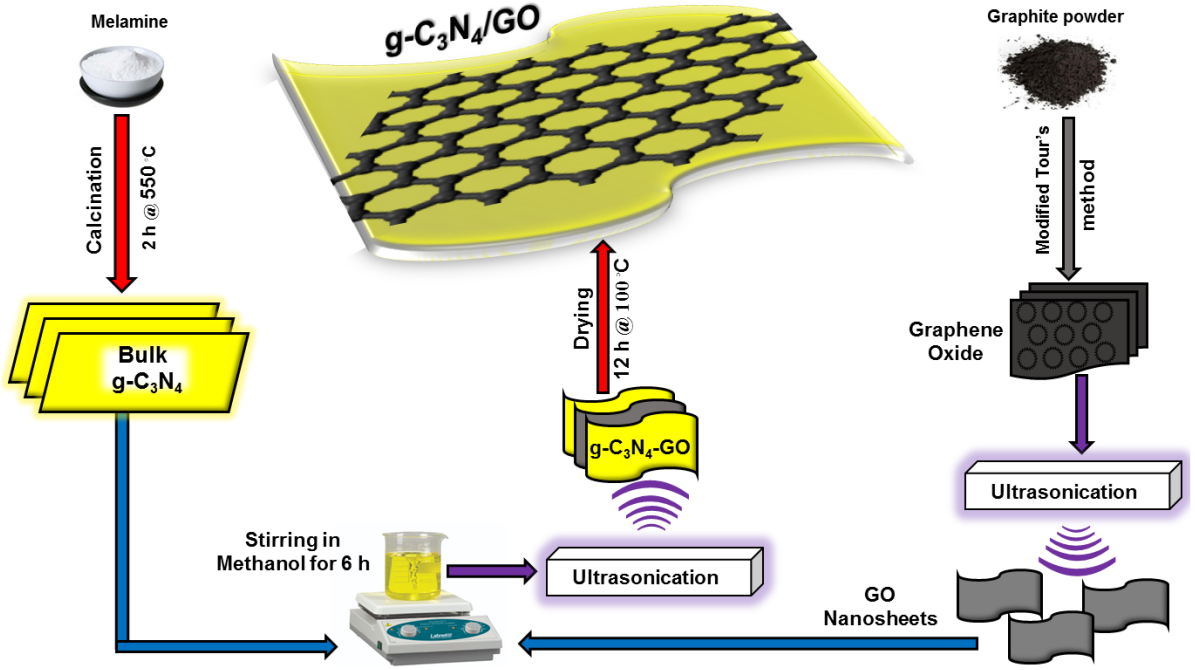

Figure 1. A schematic illustration for photo-reactor set-up used for converting the CO_2 into CH_4 under visible light.

2.5. Photocatalyst Characterizations

The crystalline phases and the crystal structure of the synthesized samples were investigated using X-ray diffraction (XRD) on D8 Bruker diffractometer operated at 40 kV voltage and 40 mA current with Cu-Kα radiation. A Hitachi SU8020 Field Emission Scanning Electron Microscope (FESEM) was employed for studying the morphologies and surfaces of the samples. However, the optical properties of the samples were characterized using UV–vis spectrophotometer (Cary 100 Agilent, Model G9821 A) while the photoluminescence (PL) analysis was conducted by Raman spectrometer (LabRAM HR Evolution, HORIBA) with a laser excitation source of 325 nm.

2.6. Photocatalytic CO_2 reduction activity and reactor set-up

The performance of the synthesized samples for converting the CO_2 gas into CH_4 was investigated using the reactor set-up displayed in Fig 2. The system consists mainly of a stainless-steel chamber fitted with an inlet and outlet valves and quartz glass window on the top. After distributing the photocatalyst powder inside the reactor chamber, pure CO_2 gas is fed into the reactor through the inlet valve after being passed through a water bubbler. The humidified CO_2 gas flows through the whole system for purging and removing any gas traces. Both inlet and outlet valves are then closed after the gas pressure is built inside the chamber. Then, the light source (Xe lamp) is switched on for starting the reaction which converts the CO2 and water molecules into CH_4 gas after a series of redox reactions. A gas product sample is drawn from the sampling point each hour using a tight gas syringe and analyzed using a gas chromatograph (Agilent GC 6890 N, USA).

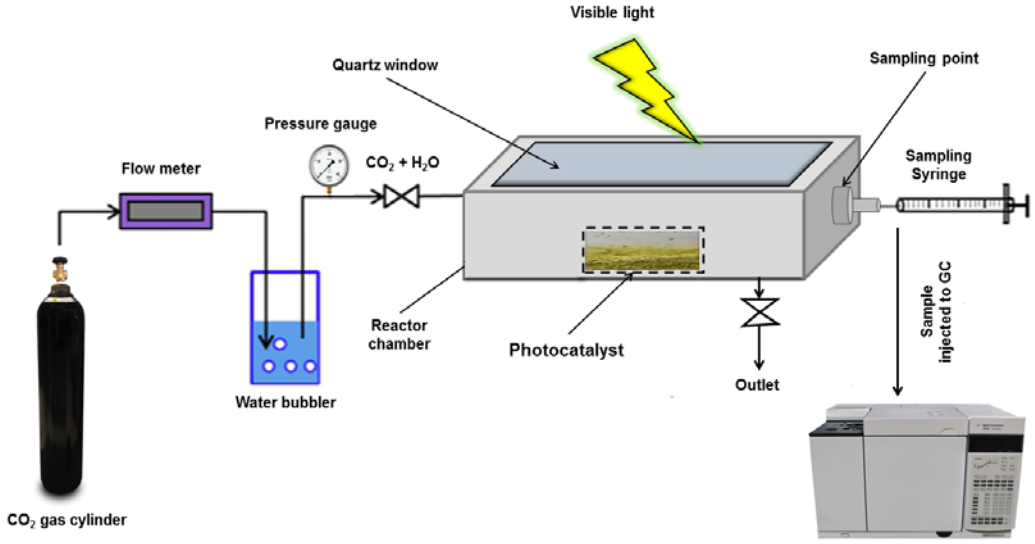

Figure 2. A scheme illustrating the photo-reactor set-up used for converting the CO_2 into CH_4 under visible light [19–21].

3. RESULTS AND DISCUSSIONS

3.1. Characterizations Analyses

3.1.1. X-ray Diffraction (XRD)

The XRD patterns of GO, g-C_3N_4 and g-C_3N_4/GO are displayed in Figure 3.

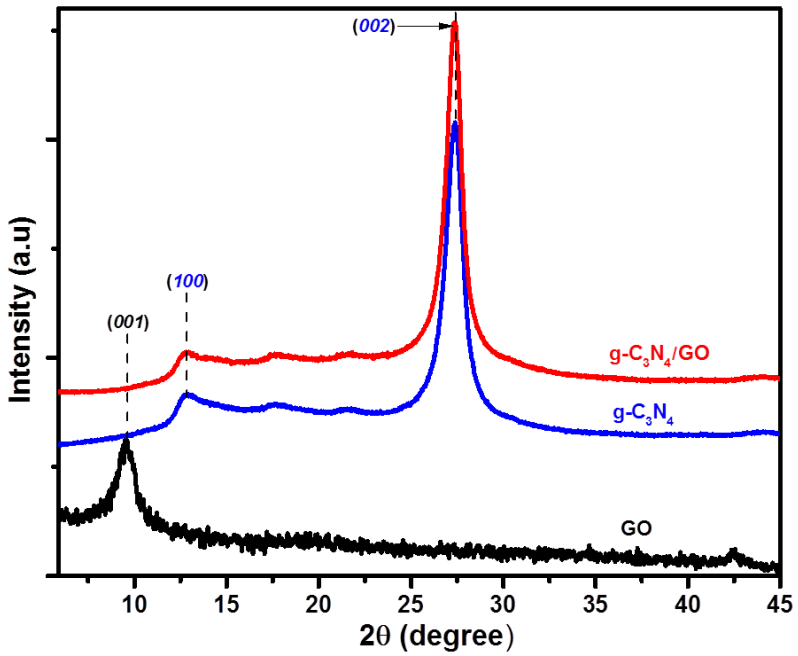

Figure 3. XRD patterns of pure of pure GO, pure g-C_3N_4 and g-C_3N_4/GO composite.

Obviously, the GO exhibited a significant peak at 2θ: 9.9° which is ascribed to the (001) GO plane of interlayer spacing [13, 22, 23]. Pure g-C_3N_4 exhibited two characteristic diffraction peaks, the

first peak at 2θ: 13° indexed to the (100) plane which belongs to the interlayer structural packing of g-C_3N_4 and the second peak at 2θ: 27.5° corresponding to the (002) diffraction plane of interlayer stacking of the aromatic system in the g-C_3N_4 [24, 25]. For the binary g-C_3N_4/GO composite, both g-C_3N_4 diffraction peaks displayed clearly while no GO peak was observed which can be ascribed to the low content of GO.

3.1.2. Field Emission Scanning Electron Microscopy (FESEM)

Figure 4 (a-c) displays the FESEM images of pristine g-C_3N_4, pure GO and g-C_3N_4/GO composite, respectively. Pure g-C_3N_4 exhibited a layered compact structure of nanosheets that are stacked together with irregular folding as shown Figure 4 (a). A large, corrugated GO nanosheet is clearly displayed in Figure 4 (b). Good interfacial contact between the nanosheets of g-C_3N_4 and GO was revealed from the FESEM images in Figure 4 (c-e). These observations have also confirmed that the synthesized photocatalysts have maintained their original 2D structure of material with no significant changes.

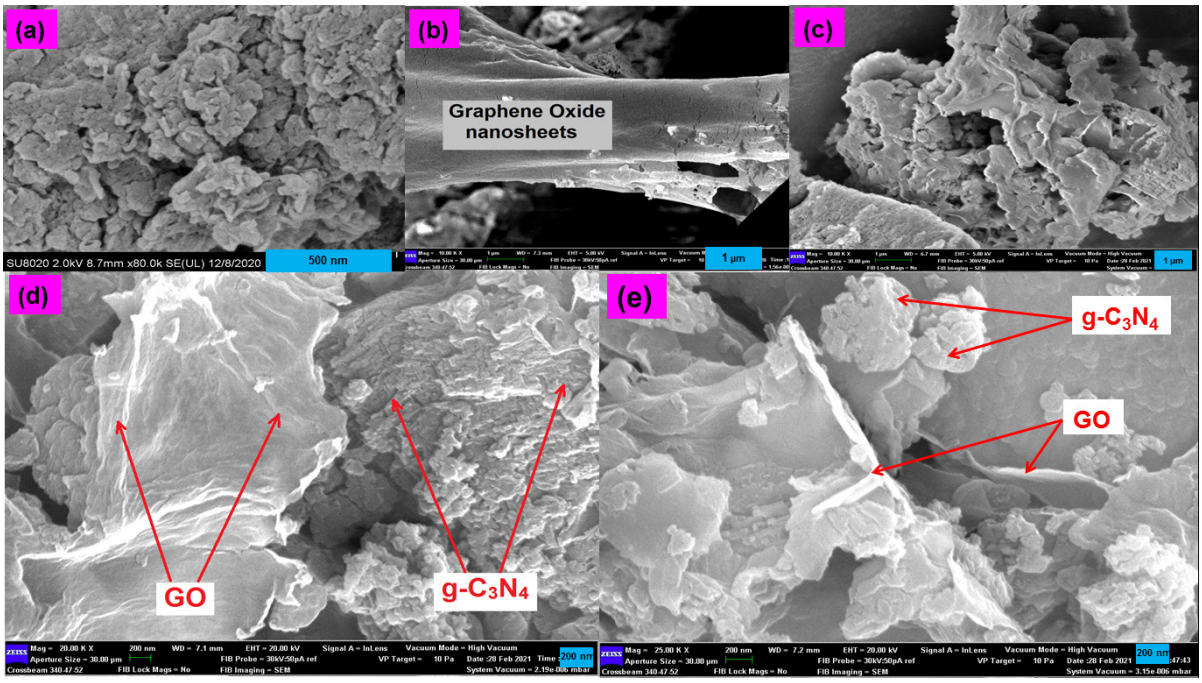

Figure 4. FESEM images of (a) pure g-C_3N_4, (b) GO nanosheet, (c-e) g-C_3N_4/GO nanocomposite at different magnifications, respectively.

3.1.3. Ultraviolet-Visible Diffuse Reflectance Spectroscopy (UV-Vis DRS)

The ability of pure g-C_3N_4 and the GO-modified g-C_3N_4 samples for absorbing light in the UV and visible range were obtained using UV-vis spectroscopy. As illustrated in Figure 5 (a), the pure g-C_3N_4 exhibited an absorption peak near 400 nm, revealing its activity in the UV-visible range, which is identical to the g-C_3N_4 optical activity reported in literature [26]. However, a significant increase in the visible light absorption was observed after adding GO. This confirms that the GO addition plays a great role in improving the light harvesting in the visible range for maximum utilization of solar light energy.

3.1.4. Photoluminescence (PL)

Generally, the photoluminescence (PL) emissions give an excellent indication for the charges recombination rate in semiconducting materials which is considered as the main challenge in the photocatalysis process [21, 27, 28]. Higher PL emissions indicate the presence of higher

recombination rate of photogenerated charges while lower emissions are more favorable for efficient charges separation and transfer. As shown in Figure 5 (b), pure g-C_3N_4 exhibited a PL spectrum with high intensity peak which is attributed to the fast charge recombination of g-C_3N_4. However, the peak was clearly reduced after coupling the g-C_3N_4 with GO, revealing the significant contribution of GO towards excellent separation efficiency of charge carriers and thus improved photocatalytic performance.

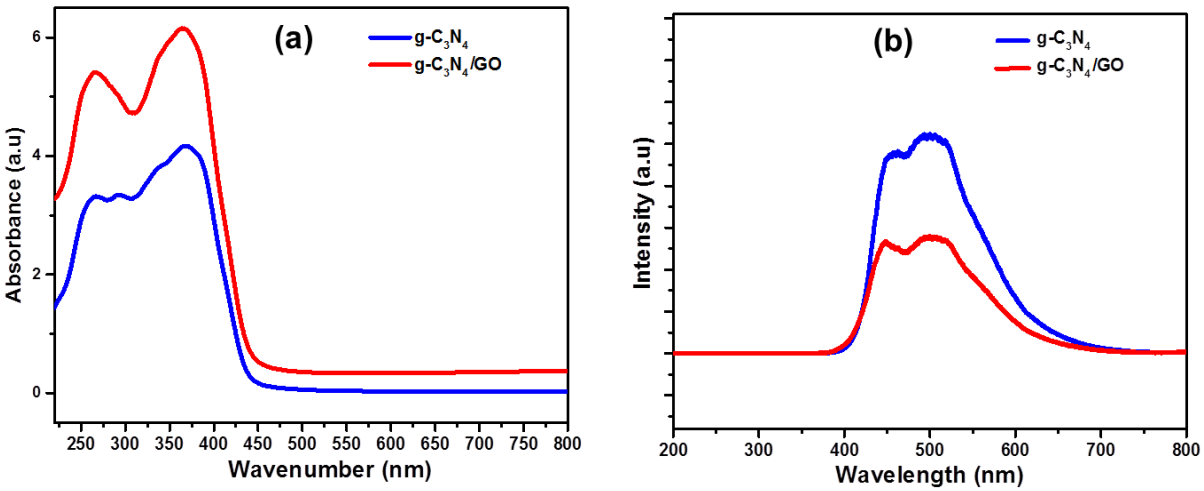

Figure 5. UV (a) and photoluminescence (PL) (b) analyses of pure g-C_3N_4 and g-C_3N_4/GO samples.

3.2. Performance of photocatalytic CO_2 reduction

The effect of modifying g-C_3N_4 with different percentages of GO (0, 0.25, 0.5, 1 and 2 wt.%) on the performance of photocatalytic CO_2 reduction to CH_4 is shown in Figure 6. It is evident that production of CH_4 was enhanced with the increase of GO content till 1%, beyond 1% GO incorporation the production of CH_4 decreased even below pure g-C_3N_4. This could possibly be explained by the effect of shielding, which lowers the amount of light that strikes the photocatalyst surface by a substantial margin [20, 29]. This is consistent with the previous study for photocatalytic H2 evolution over GO/g-C_3N_4 composite [30].

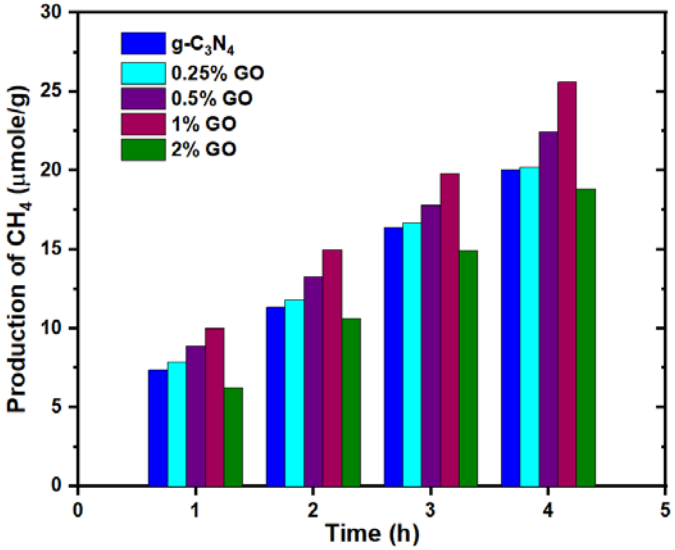

Figure 6. The effect of GO addition on the g-C_3N_4 photocatalytic performance for CO_2 reduction to CH_4.

The maximum CH_4 yield of 25.61 μmol g-1 was attained after 4 h of visible light illumination over the g-C_3N_4/GO nanocomposite photocatalyst. When compared to pure g-C_3N_4, the CH_4 yield shows a roughly 30% increase in production. The incorporation of GO into the g-C_3N_4 nanosheets contributed to the photocatalytic enhancement, as it improved the optical and structural characteristics of pure g-C_3N_4. Several other investigations supported the role of GO addition in boosting the photocatalytic performance of pure g-C_3N_4 [13, 31, 32].

4. CONCLUSION

In summary, we demonstrated the successful synthesis of 2D/2D g-C_3N_4/GO hybrid photocatalyst by applying a simple hydrothermal approach. The catalytic performance of the as constructed photocatalyst was evaluated by the CO_2 photo-reduction. The improved structural and optical properties of the heterostructure photocatalysts directed the outstanding CO_2 photo-reduction activity. The maximum CH_4 production rate of 6.4 μmol g–1 h–1 was attained after employing 0.5 wt. % GO into g-C_3N_4 nanosheets. This was substantially higher than that of pristine g-C_3N_4 (4.9 μmol g–1 h–1). The improved photocatalytic performance of the g-C_3N_4/GO heterostructure photocatalyst is attributed to the successful coupling of GO co-catalyst, which acted as a solid electron mediator and consequently facilitates the electrons transfer rate and CO_2 adsorption capability of the composite photocatalyst.

Author Contributions: Riyadh Ramadhan Ikreedeegh: Methodology, Conceptualization, Data collection, Writing-original draft, Supervision, Reviewing and Editing. Md. Arif Hossen: Software, Writing-original draft, Reviewing and Editing. Muhammad Tahir: Supervision and Funding. All authors have read and agreed to the published version of the manuscript.
Data Availability Statement: Data will be available upon request.
Funding: This research received no external funding.
Conflicts of Interest: The authors declare that they have no conflict of interest.
Acknowledgments: The authors gratefully acknowledge the United Arab Emirate University and the Arabian Gulf Oil Company for the financial support.

REFERENCES

[1] E. Gong et al., "Solar fuels: research and development strategies to accelerate photocatalytic CO_2 conversion into hydrocarbon fuels," Energy Environ. Sci., vol. 15, no. 3, pp. 880–937, 2021, doi: 10.1039/d1ee02714j.

[2] G. Centi and C. Ampelli, "CO_2 conversion to solar fuels and chemicals : Opening the new paths," J. Energy Chem., vol. 91, pp. 680–683, 2024, doi: 10.1016/j.jechem.2024.01.021.

[3] R. R. Ikreedeegh, M. Tahir, M. Madi, "Modified-TiO_2 Nanotube Arrays as a Proficient Photo-Catalyst Nanomaterial for Energy and Environmental Applications," Sol. Energy Sustain. Dev., vol. 13, no. 1, pp. 133–144, 2024, doi: https://doi.org/10.51646/jsesd.v13i1.196.

[4] V. H. Nguyen et al., "Towards artificial photosynthesis: Sustainable hydrogen utilization for photocatalytic reduction of CO_2 to high-value renewable fuels," Chem. Eng. J., vol. 402, no. June, p. 126184, 2020, doi: 10.1016/j.cej.2020.126184.

[5] R. R. Ikreedeegh and M. Tahir, "A critical review in recent developments of metal-organic-frameworks (MOFs) with band engineering alteration for photocatalytic CO_2 reduction to solar fuels," J. CO_2 Util., vol. 43, no. October 2020, p. 101381, 2021, doi: 10.1016/j.jcou.2020.101381.

[6] R. R. Ikreedeegh, M. A. Hossen, M. Tahir, and A. Abd Aziz, "A comprehensive review on anodic TiO_2 nanotube arrays (TNTAs) and their composite photocatalysts for environmental and energy applications : Fundamentals , recent advances and applications," Coord. Chem. Rev., vol. 499, no.

October 2023, p. 215495, 2024, doi: 10.1016/j.ccr.2023.215495.

[7] M. A. Hossen et al., "Recent progress in TiO_2-Based photocatalysts for conversion of CO_2 to hydrocarbon fuels : A systematic review," Results Eng., vol. 16, no. November, p. 100795, 2022, doi: 10.1016/j.rineng.2022.100795.

[8] M. A. Hossen et al., "A Comprehensive Review on Advances in TiO_2 Nanotube (TNT)-Based Photocatalytic CO_2 Reduction to Value-Added Products," Energies, vol. 15, no. 22, p. 8751, 2022, doi: https://doi.org/10.3390/en15228751.

[9] O. Ola and M. M. Maroto-valer, "Review of material design and reactor engineering on TiO_2 photocatalysis for CO_2 reduction," "Journal Photochem. Photobiol. C Photochem. Rev., vol. 24, pp. 16–42, 2015, doi: 10.1016/j.jphotochemrev.2015.06.001.

[10] A. A. Khan and M. Tahir, "Recent advancements in engineering approach towards design of photo-reactors for selective photocatalytic CO_2 reduction to renewable fuels," J. CO_2 Util., vol. 29, no. May 2018, pp. 205–239, 2019, doi: 10.1016/j.jcou.2018.12.008.

[11] D. Zhou, J. Zhang, Z. Jin, T. Di, and T. Wang, "Reduced graphene oxide assisted g-C_3N_4/rGO/NiAl-LDHs type II heterostructure with high performance photocatalytic CO_2 reduction," Chem. Eng. J., vol. 450, no. P3, p. 138108, 2022, doi: 10.1016/j.cej.2022.138108.

[12] D. Xu, B. Cheng, W. Wang, C. Jiang, and J. Yu, "Ag2CrO4/g-C_3N_4/graphene oxide ternary nanocomposite Z-scheme photocatalyst with enhanced CO_2 reduction activity," Appl. Catal. B Environ., vol. 231, no. March, pp. 368–380, 2018, doi: 10.1016/j.apcatb.2018.03.036.

[13] R. Ramadhan and M. Tahir, "Facile fabrication of well-designed 2D/2D porous g-C_3N_4–GO nanocomposite for photocatalytic methane reforming (DRM) with CO_2 towards enhanced syngas production under visible light," Fuel, vol. 305, no. March, p. 121558, 2021, doi: 10.1016/j.fuel.2021.121558.

[14] C. Prasad, N. Madkhali, V. Govinda, H. Yeol, and I. Bahadur, "Recent progress on the development of g-C_3N_4 based composite material and their photocatalytic application of CO_2 reductions," J. Environ. Chem. Eng., vol. 11, no. 3, p. 109727, 2023, doi: 10.1016/j.jece.2023.109727.

[15] Q. Guo et al., "Improved photocatalytic activity of porous ZnO nanosheets by thermal deposition graphene-like g-C_3N_4 for CO_2 reduction with H2O vapor," Appl. Surf. Sci., vol. 509, no. August 2019, p. 144773, 2020, doi: 10.1016/j.apsusc.2019.144773.

[16] X. Li et al., "Local surface plasma resonance effect enhanced Z-scheme ZnO/Au /g-C_3N_4 film photocatalyst for reduction of CO_2 to CO," Appl. Catal. B Environ., vol. 283, no. October 2020, p. 119638, 2021, doi: 10.1016/j.apcatb.2020.119638.

[17] Z. Li et al., "Boosting the photocatalytic CO_2 reduction activity of g-C_3N_4 by acid modification," Sep. Purif. Technol., vol. 338, no. January, p. 126577, 2024, doi: 10.1016/j.seppur.2024.126577.

[18] C. Prasad et al., "An overview of graphene oxide supported semiconductors based photocatalysts : Properties , synthesis and photocatalytic applications," J. Mol. Liq., vol. 297, p. 111826, 2020, doi: 10.1016/j.molliq.2019.111826.

[19] M. A. Hossen et al., "Enhanced Photocatalytic CO_2 Reduction to CH4 Using Novel Ternary Photocatalyst RGO/Au-TNTAs," Energies, vol. 16, no. 14, 2023, doi: 10.3390/en16145404.

[20] R. R. Ikreedeegh and M. Tahir, "Indirect Z-scheme heterojunction of NH2-MIL-125 (Ti) MOF/g-C_3N_4 nanocomposite with RGO solid electron mediator for efficient photocatalytic CO_2 reduction to CO and CH4," J. Environ. Chem. Eng., vol. 9, no. 4, p. 105600, 2021, doi: 10.1016/j.jece.2021.105600.

[21] R. R. Ikreedeegh and M. Tahir, "Ternary nanocomposite of NH2-MIL-125(Ti) MOF-modified TiO_2 nanotube arrays (TNTs) with GO electron mediator for enhanced photocatalytic conversion of CO_2 to solar fuels under visible light," J. Alloys Compd., vol. 969, no. October, p. 172465, 2023, doi: 10.1016/j.jallcom.2023.172465.

[22] R. R. Ikreedeegh, S. Tasleem, and M. A. Hossen, "Facile fabrication of binary g-C_3N_4/

NH2-MIL-125 (Ti) MOF nanocomposite with Z-scheme heterojunction for efficient photocatalytic H 2 production and CO_2 reduction under visible light," Fuel, vol. 360, no. PC, p. 130561, 2024, doi: 10.1016/j.fuel.2023.130561.

[23] T. Kuilla, S. Bhadra, D. Yao, N. Hoon, S. Bose, and J. Hee, "Progress in Polymer Science Recent advances in graphene based polymer composites," Prog. Polym. Sci., vol. 35, no. 11, pp. 1350–1375, 2010, doi: 10.1016/j.progpolymsci.2010.07.005.

[24] N. Cao and Y. Zhang, "Study of Reduced Graphene Oxide Preparation by Hummers 'Method and Related Characterization," J. Nanomater., vol. 2015, pp. 1–5, 2015, doi: 10.1155/2015/168125.

[25] J. Liu, T. Zhang, Z. Wang, G. Dawson, W. Chen, "Simple pyrolysis of urea into graphitic carbon nitride with recyclable adsorption and photocatalytic activity †," J. Mater. Chem., vol. 21, pp. 14398–14401, 2011, doi: 10.1039/c1jm12620b.

[26] S. Tasleem and M. Tahir, "Constructing LaxCoyO3 Perovskite Anchored 3D g-C_3N_4 Hollow Tube Heterojunction with Pro fi cient Interface Charge Separation for Stimulating Photocatalytic H2 Production," Energy and Fuels, vol. 35, pp. 9727–9746, 2021, doi: 10.1021/acs.energyfuels.1c00512.

[27] R. R. Ikreedeegh and M. Tahir, "Photocatalytic CO_2 reduction to CO and CH4 using g-C_3N_4/RGO on titania nanotube arrays (TNTAs)," J. Mater. Sci., vol. 56, no. 34, pp. 18989–19014, 2021, doi: 10.1007/s10853-021-06516-7.

[28] R. R. Ikreedeegh, M. Tahir, "Titanium Carbide (TiC) MXene-Based Titanium Dioxide Composites for Energy and Environment Applications," in Titanium Carbide MXenes: Synthesis, Characterization, Energy and Environmental Applications, Wiley, 2024, pp. 87–114.

[29] W. He et al., "Controllable morphology $CoFe_2O_4$/g-C_3N_4 p-n heterojunction photocatalysts with built-in electric field enhance photocatalytic performance," Appl. Catal. B Environ., vol. 306, no. December 2021, p. 121107, 2022, doi: 10.1016/j.apcatb.2022.121107.

[30] J. Li et al., "Ultrasonic-microwave assisted synthesis of GO/g-C_3N_4 composites for efficient photocatalytic H2 evolution," Solid State Sci., vol. 97, no. August, p. 105990, 2019, doi: 10.1016/j.solidstatesciences.2019.105990.

[31] K. Prakash, S. Karuthapandian, and C. Cv, "Construction of Novel Metal - Free Graphene Oxide / Graphitic Carbon Nitride Nanohybrids : A 2D–2D Amalgamation for the Effective Dedyeing of Waste Water," J. Inorg. Organomet. Polym. Mater., vol. 31, no. 2, pp. 716–730, 2021, doi: 10.1007/s10904-020-01728-x.

[32] Shalu Guptaa and Rakesh Kumar, "Enhanced photocatalytic performance of the N-rGO/g-C_3N_4 nanocomposite for efficient solar-driven water remediation," Nanoscale, vol. 16, pp. 6109–6131, 2024, doi: 6109-6131.